

Semi-Active Pulse-Switching SSDC Vibration Suppression using Magnetostrictive Materials

S. Mohammadi, S. Hatam^{*}, A. Khodayari

Mechanical Engineering Department, Razi University, Kermanshah, Iran

Received 11 July 2019; accepted 12 September 2019

ABSTRACT

One of the best vibration control methods using smart actuators are semi-active approaches which are as strong as active methods and need no external energy supply such as passive ones. Compared with piezoelectric-based, magnetostrictive-based control methods have higher coupling efficiency, higher Curie temperature, higher flexibility to be integrated with curved structures and no depolarization problems. Semi-active methods are well developed for piezoelectrics but magnetostrictive-based approaches are not as efficient, powerful and well known as piezoelectric-based methods. The aim of this work is to propose a powerful semi-active control method using magnetostrictive actuators. In this paper a new type of semi-active suppression methods using magnetostrictive materials is introduced which contains an equipped vibrating structure with magnetostrictive patches wound by a pick-up coil connected to an electronic switch and a capacitor. The novelty of the proposed damping method is switching on the coil current signal using mentioned switch and capacitor, which is briefly named SSDC (synchronized switch damping on capacitor). In this paper, the characteristics of the semi-active pulse-switching damping technique with magnetostrictive materials are studied and numerical results show significant damping for almost all types of excitations.

© 2019 IAU, Arak Branch. All rights reserved.

Keywords: Pulse-switching; Magnetostrictive materials; Semi-active; Vibration control.

1 INTRODUCTION

VIBRATION damping is one of the manifestations of mechanical energy dissipation related to motion in mechanical systems. Sometimes just changing the system's stiffness or mass to alter the resonance frequencies can reduce unwanted vibrations as long as the excitation frequency does not change. But in most cases, vibrations need to be dissipated using damping materials or devices tunable with vibrations. Several methods have been investigated for vibration damping. These methods are passive, active and semi-active treatments that can be used

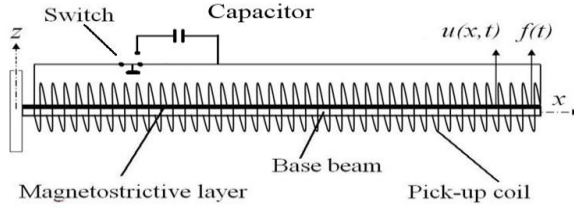
^{*}Corresponding author. Tel.: +98 9183853920.
E-mail address: salar.hatam@yahoo.com (S. Hatam).

for sound/vibration cancellation. Active control involves the use of active elements (actuators) along with sensors and controllers (analogue or digital) to produce an out of phase actuation to cancel the disturbance causing the noise/vibration [1]. All other methods that do not include a real-time active algorithm can be grouped under the passive control option. Passive damping refers to energy dissipation within the structure by add-on damping devices. Viscous dampers (dashpots), viscoelastic damping, tuned-mass dampers, dynamic absorbers and shunted piezoelectric dampers are the mechanisms of passive vibration control. The most common types of passive damping treatments using viscoelastic materials are described by Rao [2]. Semi-active approaches have experienced significant developments in recent years. In these techniques, required energy for vibration suppression is extracted from the vibrating structure itself. Used materials play a very important role in the efficiency of this technique. Smart materials such as piezoelectric ceramics and polymers are classes of materials that can be used as actuators for energy conversion. Piezoelectric materials are probably the best developed and best understood of all smart materials. They are widely used as sensors and actuators in vibration and noise control of the smart structures because of their excellent frequency characteristics and capabilities in reciprocal conversion between electric and mechanical strain energy [3-8]. The use of piezoelectricity has increased much faster in modern engineering processes. Functionally graded material (FGM) is of great use in several manufacturing process. To satisfy the requirements of modern technologies and material science, functionally graded piezoelectric material (FGPM) was discovered in the line of FGMs [9]. Piezomagnetic (PM) materials are one of the advanced composite materials in which the magnetic effect is generated by applying mechanical stress. Similarly, in piezoelectric (PE) materials, the electric charge gets accumulated and induced electricity in response to applied physical stress. PE/PM material composites are used to manufacture the actuators, rotating sensors, acoustic devices, control sensors, and transducers [10]. They can transform electrical energy into magnetic energy and vice-versa. Such a one experienced process is known as magnetoelectric (ME) effect, that phenomenon occurs from the combination of two distinct phases through interfaces and is absent in every phase [11]. In Piezoelectric materials, some disadvantages such as depolarization and charge leakage, affect their applications. Also, piezoelectric materials are very brittle and cannot endure large strains. Magnetostrictive materials (MsMs) as a class of metallic compounds has been recently considered in application of vibration control. With the development of giant MsMs and metallic glass in the last decade, MsMs have been increasingly applied in a wide variety of smart structures. It utilizes the Joule effect, where the changes in magnetization of the material induces strain of MsM consequently upon dynamic or cyclic loading; this strain can be used for vibration control as an actuator [12-16]. Magnetostrictive actuators in comparison with other actuators produce higher forces and relatively high deformations. These properties make them suitable for different vibration control applications [17-21]. Recently, some researches have been done on the magnetosrective actuators for vibration suppression [20, 22, 23]. Compared with piezoelectric based, MsM-based has higher coupling efficiency (>0.9), higher Curie temperature, higher flexibility to be integrated with curved structures, and no depolarization problem (because magnetostriction is an inherent material property) [24]. Thus, it can be used for almost unlimited vibration cycles with significantly enhanced reliability. However, it has relatively large dimensions, which is hard to be integrated with small structures, because of the pick-up coil.

In this paper a new technique of semi-active pulse-switching vibration suppression using MsMs is proposed in which vibration suppression occurs with synchronized switching on a constant capacitor connected to the electro-mechanical system. Indeed, the novelty of the proposed method is introducing SSDC (synchronized switch damping on capacitor) switching strategy. In the following a theoretical model of MsM layer attached to a vibrating cantilever beam wound by a pick-up coil is considered. Because of deformation of the MsM layer, a current will be induced in the coil. The proposed damping method is described in the switching strategy section in the following. When the switch triggers on the selected extremums of the coil current, the electrical current charges a capacitor, then the capacitor produces a negative current in the reverse direction because of the coil inductance motivation. This current flows back into the coil and produces an out of phase damping force with displacement signal. In order to damp any type of vibration, statistical analysis of the structural deflection to predict the optimum instants for switching sequences, is implemented in this study [5]. It should be mentioned that the switch is closed during the half period of LC circuit. Different excitation types have been controlled using the proposed technique and numerical results are presented in the following.

2 THEORETICAL MODELING OF MAGNETO-MECHANICAL SYSTEM

A prototype of the MsM device has been proposed with metglas 2605SC laminate bonded on a cantilever aluminum beam wound by a pick-up coil (Fig. 1).

**Fig.1**

Schematic diagram of the cantilever beam consisting of aluminum base beam and a metglas ribbon wound by a pick-up coil and also attached SSDC control circuit. $u(x,t)$ is the beam deflection along the transverse direction (z) and $f(t)$ is the external excitation.

The differential equation for a cantilever beam with lateral motion excited by an external force is specified as [25]:

$$\rho \frac{\partial^2 u(x,t)}{\partial t^2} + c \frac{\partial u(x,t)}{\partial t} + \frac{\partial^2}{\partial x^2} [EJ \frac{\partial^2 u(x,t)}{\partial x^2}] = f(x,t), \quad f(x,t) = p(x)f(t) \quad (1)$$

where $u(x,t)$ is the lateral beam deflection, E and J represent Young's modulus and the inertia moment of the cross-section. ρ , c and $f(x,t)$ are the mass, damping and the excitation force per unit length, respectively. $p(x)$ is the load's spatial distribution and $f(t)$ is the input time history. This equation corresponds to Euler-Bernoulli assumptions. In addition, we assume that the particular solution is as the following:

$$u(x,t) = \sum_{i=1}^n \varphi_i(x) q_i(t) \quad (2)$$

where $q_i(t)$ and $\varphi_i(x)$ are the modal coordinates and the Eigen mode functions respectively and n is the number of modes. The Eigen mode functions are orthogonal and satisfy the following relations:

$$\int_0^l \rho \varphi_i(x) \varphi_k(x) dx = \begin{cases} 0 & \text{for } i \neq k \\ M_i & \text{for } i = k \end{cases}$$

$$\int_0^l \frac{d^2}{dx^2} [EJ \frac{d^2 \varphi_i(x)}{dx^2}] \varphi_k(x) dx = \begin{cases} 0 & \text{for } i \neq k \\ K_i & \text{for } i = k \end{cases} \quad (3)$$

$$\int_0^l c(x) \varphi_i(x) \varphi_k(x) dx = \begin{cases} 0 & \text{for } i \neq k \\ c_i & \text{for } i = k \end{cases}$$

where M_i , K_i and c_i are the generalized mass, stiffness and damping coefficients for the i th mode and l is the cantilever beam length. Substituting of Eq. (2) in Eq. (1) and multiplying it by $\varphi_k(x) dx$, then integrating on length l and employing the orthogonality conditions of Eq. (3); and if the damping be proportional to the mass and stiffness distributions, the result is:

$$M_i \ddot{q}_i + c_i \dot{q}_i + K_i q_i = \bar{Q}_i f(t), \quad \bar{Q}_i = \int_0^l p(x) \varphi_i(x) dx \quad (4)$$

where $q_i(t)$ can be determined from these equations and \bar{Q}_i is the generalized excitation force [25]. For the cantilever beam problem depicted in Fig. 1 equipped by a metglas 2605 SC laminate wound by a pick-up coil, excited by an external force at the free end and considering linear constitutive equation for MsM and in conjunction with normal mode superposition method based on the Euler-Bernoulli beam theory; Eq. (4) can be rearranged as:

$$M_i \ddot{q}_i + c_i \dot{q}_i + K_i q_i = \bar{Q}_i f(t) - G_i i_i(t) \quad (5)$$

The term $G_i i_i(t)$ corresponds to the force due to i th component of the current; according to the macroscopic metglas coefficient G_i . Metglas constitutive equation (Eq. (6)), mechanics of materials relations (Eq. (8)) and electromagnetic equations (Eq. (9)) are as the following:

$$\begin{aligned} S &= s^H \sigma + dH \\ B &= d^* \sigma + \mu^\sigma H \end{aligned} \quad (6)$$

where,

$$d = \left. \frac{\partial S}{\partial H} \right|_{\sigma}, \quad d^* = \left. \frac{\partial B}{\partial \sigma} \right|_H \quad (7)$$

For small strains, d and d^* are considered to be equal.

$$\dot{S} = -z \frac{\partial^2 \dot{u}(x, t)}{\partial x^2} \quad (8)$$

$$H = \frac{Ni}{l} \quad (9)$$

where σ and S are the mechanical stress and strain respectively. H and B are the magnetic field intensity and flux density. μ^σ is the permeability of the core material of the coil under constant stress, s^H is the elastic compliance under constant magnetic field, N is the number of the pick-up coil turns and i is the current. Indeed, the constitutive Eqs. (6) are extended to the macro-behavior model of the MsM device with a cantilever beam and a pick-up coil. It is assumed that both aluminum beam and metglas laminate have the same width b and length l . Faraday's law relating the voltage to the infinitesimal portion of the coil dx is as the following:

$$dv = -\frac{N}{l} A_M \dot{B} dx \quad (10)$$

where $A_M = bt_M$ is the cross sectional area of the metglas laminate. t_M and v are the metglas laminate thickness and electrical voltage, respectively. Inserting Eq. (2) into (8), then Eqs. (8), (9) and (10) into the time derivative of the second equation of Eq. (6) and integrating the resulting equation with respect to x leads to:

$$v = \sum_{i=1}^n G_i \dot{q}_i - L_e \dot{i} \quad (11)$$

where G_i and L_e are as the following [26]:

$$G_i = \frac{Nd^* E^H A_M h_M}{l} \int_0^l \phi_i''(x) dx \quad (12)$$

$$L_e = \frac{\mu^S N^2 A_M}{l} \quad (13)$$

h_M is the distance from the centroid of the metglas laminate to the neutral axis. E^H is the Young's modulus of the MsM under constant magnetic field, L_e is the equivalent inductor associated with the coil wound around the metglas laminate and μ^S is the MsM permeability under constant strain. Finally by solving Eqs. (5) and (11) together, beam displacement in controlled case is obtainable.

In order to compare this control approach with uncontrolled case, it is necessary to define the evaluation parameters. The used quantity is related to the deflection of the structure. This quantity I_u , which is a summation in the time variable for the considered modes, is the mean squared response of $u(x, t)$ [25] and is defined as:

$$I_u = \overline{u(x, t)^2} = \lim_{\tau \rightarrow \infty} \left(\frac{1}{\tau} \int_0^\tau u^2(x, t) dt \right) = \sum_i \sum_k \left[\phi_i(x) \phi_k(x) \lim_{\tau \rightarrow \infty} \left(\frac{1}{\tau} \int_0^\tau q_i(t) q_k(t) dt \right) \right] \quad (14)$$

The displacement damping A_u is then evaluated as:

$$A_u = 10 \log \left(\frac{(I_u)_{\text{controlled}}}{(I_u)_{\text{uncontrolled}}} \right) \quad (15)$$

3 SSDC SWITCHING STRATEGY

The principles of SSDC technique consist of adding an electronic switch in series with a capacitor and a magneto-mechanical generator that causes an inversion of the produced current in the selected extremums of the mechanical deflection. In order to better understanding of the performance of the semi-active SSDC control technique, a driven series RLC circuit with an AC generator is assumed. Considering the behavior of current and voltage of the electronic elements, the instantaneous voltages across each of the three circuit elements R , L and C have different amplitudes and phases compared to the current, as shown in Fig. 2. The current phasor I leads the capacitive voltage phasor V_C by $\pi / 2$ but lags the inductive voltage phasor V_L by $\pi / 2$ (V_R is the resistive voltage phasor) [27]. The three voltage phasors rotate counter-clockwise as time increases, with their fixed relative positions.

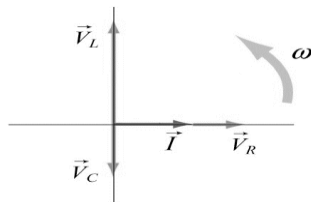


Fig.2
Phasor diagram for the series RLC circuit.

In SSDC pulse-switching technique, the pick-up coil is always short-circuited that a current corresponding to the beam deflection flows into the circuit. At selected extremums of the deflection signal and when the circuit current reaches its maximum value, switch triggering occurs and an oscillating electrical RLC circuit is established. The electrical oscillation period is chosen much smaller than the mechanical period. R is the equivalent resistance of the circuit. The switch turns to the short circuit after a half period of RLC circuit, resulting an inversion of the pickup coil current. Indeed, the switch is hold connect to the capacitor until the current inverts completely. Just after the switch triggering moment, suddenly a maximum current of electrical charge flows in the RLC circuit. At this time, the voltage across the equivalent inductor and the capacitor is zero. The phasor diagram of the RLC circuit just after the switch triggering, by considering electronic elements behavior is shown in Fig. 3(a). Now, the electrical current charges the capacitor and the voltage across the capacitor starts to rise up and the circuit current decreases to zero. Simultaneously, negative voltage across the equivalent inductor increases. Therefore, the phasor diagram of the circuit turns counter-clockwise and when the capacitor is charged and the current is zero, the phasor diagram is similar to Fig. 3(b). Capacitor charging process occurs during the first quarter of the RLC electric circuit period. Then, because of negative voltage of the inductor, the electric charge stored on the capacitor flows in the circuit in the reverse direction and a negative current goes into the coil producing a resistive force in the reverse direction of the beam deflection. It is similar to Coulomb damping force. Then, the capacitor discharges in the second quarter of the RLC electric circuit period. The phasor diagram of the circuit just after the capacitor discharging process is shown in Fig. 3(c). Just after the capacitor discharging, the electronic switch turns to the short circuit case. In Fig. 3, V_{Le} and L_e are the voltage and equivalent inductance of the pick-up coil, respectively.

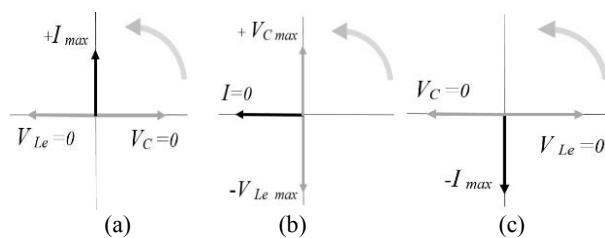


Fig.3
Phasor diagram for the series RLC circuit in SSDC switching technique, (a) just after the switch triggering, current is maximum, (b) just before the negative current flow, current is zero and the capacitor has been charged, (c) capacitor is discharged, current is maximum in the reverse direction.

4 SSSC SWITCHING INSTANT

In the case of harmonic vibrations, switching should occur on each extremum of the current signal. But, in random vibrations, the beam deflection should reach a significant value before switch triggering. In this case, the statistical analysis of current signal is used to predict suitable switching instant. The statistical strategy is based on the idea that allows the signal to reach a significant value before allowing switch triggering [5], in which the energy stored on the magneto-mechanical generator is higher. In this case, in each instant, the deflection signal $u(t)$ is studied during a given time window T_{es} just before the present time (a moving sliding time window on the signal) and statistically probable deflection threshold u_m is determined from both the temporal average μ_u and standard deviation σ_u of the signal during the observation period T_{es} . Then, it is compared to the observation signal to define the instant of the next switch. The positive deflection threshold u_m will be derived as:

$$u_m = \left| \mu_u \right| + \gamma \sigma_u \quad (16)$$

where γ is an arbitrary coefficient. According to statistical-based switch triggering, once the deflection reaches a significant and statistically probable value, switching will occur in SSSC circuit when the absolute value of the deflection reaches the threshold u_m (switching condition $|u(t)| > u_m$), causing current inversion in the circuit (Fig. 4).

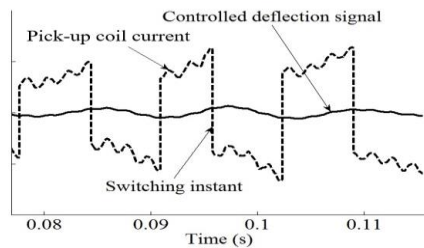


Fig.4
Strategy of SSSC pulse switching technique.

5 FREQUENCY BOUND ENHANCEMENT

In general, vibration damping using smart materials such as piezoelectrics, magnetostrictives etc. are strong in low frequency vibrations and by frequency increasing, damping efficiency decreases significantly. Therefore, adding a passive damping layer to the vibrating structure that is strong in high frequencies completes the proposed method damping ability. Using a PCLD (passive constrained layer damping) layer attached to the beam surface, in addition to the proposed SSSC damping method will give a complete control technique in both low and high frequency bands. The assumed PCLD layer contains a viscoelastic layer and an aluminum constraining layer. The viscoelastic layer possesses both elastic and viscous (linear anelastic) properties which may be modelled as an infinite number of possible configurations of elastic springs and viscous dashpots (Kelvin-Voigt model) [28-30]. For a thick beam with a thin constraining layer, it can be assumed that the thick beam dominates the flexural rigidity of the system. Then, the equipped beam vibrates in the same mode of the simple beam [31]. An important structural parameter for each material is the loss factor (η) which is defined as [32]:

$$\eta = 2\zeta \quad (17)$$

where ζ is the damping ratio. Therefore, the next step is the equipped beam loss factor evaluation in order to find the equivalent-damping ratio of the system. The most effective element on this factor is the attached viscoelastic layer. Viscoelastic materials properties are defined in the complex domain, a real part associated with the elastic behaviour and an imaginary part associated with the viscous behaviour of the material. Viscoelastic complex shear modulus is generally modeled as [33]:

$$G^* = G' + iG'' = G'(1 + i\eta_r) \quad (18)$$

where the real part is called the storage modulus and the imaginary part is called the loss modulus. The viscoelastic

loss factor (η_v) is the ability of a viscoelastic polymer to dissipate energy and generally is used to describe damping characteristics of viscoelastic polymers.

An estimation of the maximum loss factor of the equipped beam can be calculated using a simple single degree of freedom (SDOF) lumped parameter model (Fig. 5) [34]. The analysis begins by considering a model of a spring (k_o) in parallel with spring (k_l) and spring (k_v) as shown in Fig. 5. Spring k_o is the representative of the structure and k_l and k_v represent the elastic constraining layer and the viscoelastic material respectively. The maximum loss factor in the SDOF system is as the following [34]:

$$\eta_{tot(max)} = \frac{\eta_v r}{2 + r + 2\sqrt{(1 + \eta_v^2)(r + 1)}} \quad , \quad r = \frac{k_o + k_l}{k_o} - 1 \quad (19)$$

Then the damping ratio of the equipped beam can be obtained using Eqs. (17) and (19). Boundary conditions have no significant effect on the loss factor, so the explained method can be applied to any composite beam configuration such as simply supported, cantilever etc. [31].

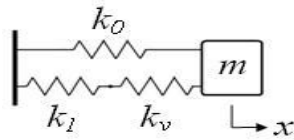


Fig.5
SDOF model of a viscoelastically damped system [34].

6 NUMERICAL RESULTS

The numerical sample is an aluminum cantilever beam equipped with a metglas ribbon on one side wound by a pickup coil (Fig. 1) under an external excitation at the free end of the beam. The other side of the beam is covered by a PCLD layer. Metglas magnetization changes under the excitation force. This change in magnetization induces a current in the pick-up coil. Passive damping of the added PCLD layer is generated mainly by shear stresses in the viscoelastic layer. In this case, viscoelastic core is strongly deformed in the shear mode due to the effect of the constraining layer. The model (Eqs. (5), (11), (17) and (19) principally) is simulated by the numerical integration using the fourth-order Runge-Kutta algorithm. The simulations are carried out using the statistical pulse-switching technique described previously. The considered signal for the threshold definition is the beam deflection $u(t)$. The observation time window T_{es} has to be twice the period of the lowest natural frequency in order to give satisfactory results. This time should be sufficiently long to obtain a realistic image of the deflection, especially for the lowest frequency mode and sufficiently short to maintain a good frequency response using the control method.

The considered structure (Fig. 1), corresponding numerical data and system modal parameters are gathered in Tables 1, 2, 3 and 4. Number of pick-up coil turns is 300 and the internal resistance of the inductance and electronic switch is 1Ω . Harmonic excitations with the frequencies corresponding to the first, second and the third natural modes of the equipped beam and also stationary and non-stationary random excitations, random shock and pulse excitations are applied to the free end of the beam and the results are presented in the following.

Table 1

Mechanical characteristics of the base beam [35].

Base beam	Aluminum, $180 \times 90 \times 2 \text{ mm}$
Young's modulus (E_b)	70 Gpa
Damping ratio (ζ)	0.002
Density	2700 kg/m^3

Table 2

Mechanical and electromagnetic characteristics of the magnetostrictive layer [26, 36].

Material and dimensions	Metglas 2605 SC, $180 \times 90 \times 0.3 \text{ mm}$
Density	7320 kg/m^3
Young's modulus (E^H)	$25\text{-}200 \text{ Gpa}$
Metglas coefficient (d)	$400 \times 10^{-9} \text{ m/A}$
Permeability - annealed (μ^S)	0.3768 H/m

Table 3

Mechanical characteristics of the PCLD layer.

Constraining layer (material and dimensions)	Aluminum 180×90×0.1 mm
Viscoelastic layer	ISD-112
Young's modulus of the constraining layer (E_c)	70 Gpa
Loss factor of the constraining layer (η_c)	0.004

Table 4

Modal parameters of the beam equipped with metglas and PCLD layers.

	Frequency (Hz)	G (N/A) – [2605 SC] computed from Eq. (12)	k_0 (N/m)	k_1 (N/m)
1 st bending mode	78	511	0.0131×10^6	0.0133×10^5
2 nd bending mode	495	1658	0.5332×10^6	0.5442×10^5
3 rd bending mode	1364	2996	4.0093×10^6	4.0921×10^5

Fig. 6 shows the non-stationary random and random shock excitations.

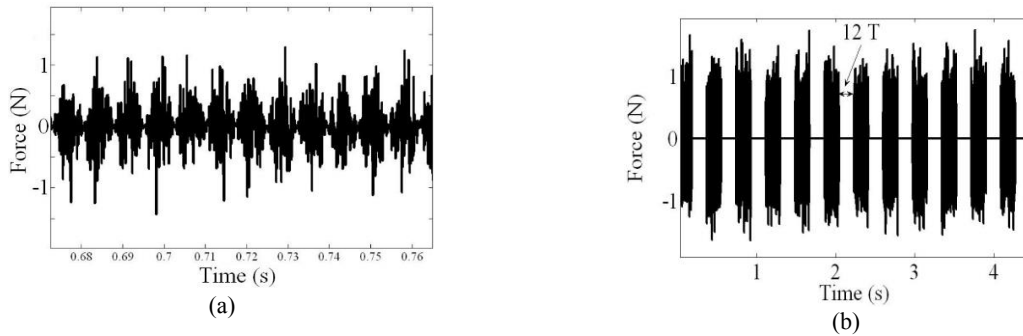


Fig.6

(a) Non-stationary. (b) Random shock excitations.

Figs. 7 to 9 illustrate the beam tip displacement with and without SSDC (without PCLD layer) control method, for non-stationary random, random shock and rectangular pulse of white noise (pulse duration is 0.006 s) excitations, respectively. The time duration of each excitation force is equal to 300 times of the longest natural period of the mechanical system. The stationary random excitation is a Gaussian white noise with constant mean value and the non-stationary random is a Gaussian white noise with variable mean value. Random shock is a non-stationary random signal shaped in time by a rectangular envelope function, which appears as a pulse of white noise shaped as a rectangle. Resulted damping for mentioned excitation is shown in the Fig. 10. As shown in Figs. 7 to 10, the performance of the proposed SSDC technique is remarkable and resulted damping are significant for almost any type of excitations.

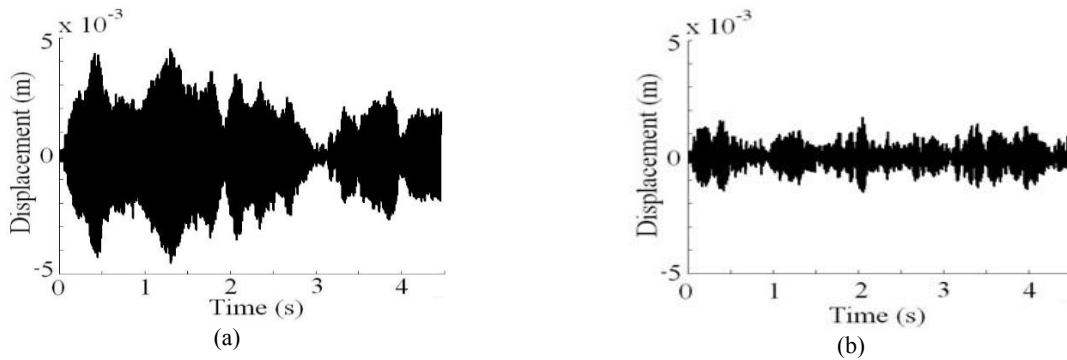


Fig.7

Cantilever beam tip displacement under non-stationary random excitation, (a) uncontrolled (b) SSDC controlled.

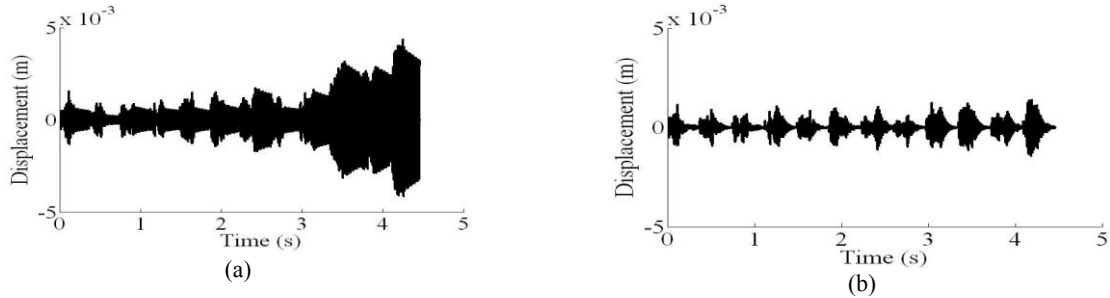


Fig.8 Cantilever beam tip displacement under random shock excitation, (a) uncontrolled (b) SSDC controlled.

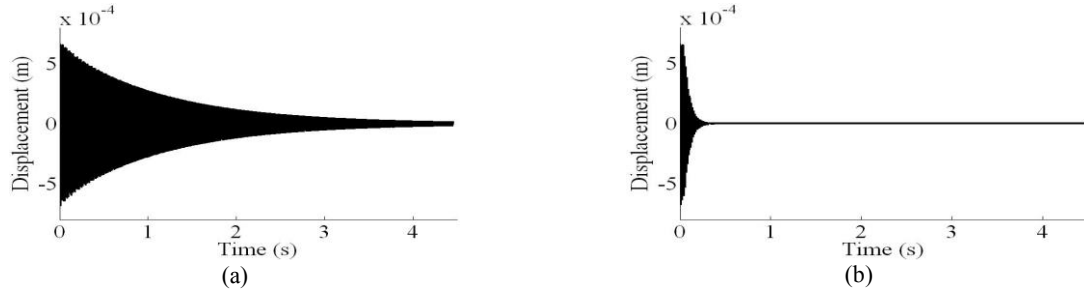


Fig.9 Cantilever beam tip displacement under rectangular pulse excitation, (a) uncontrolled (b) SSDC controlled.

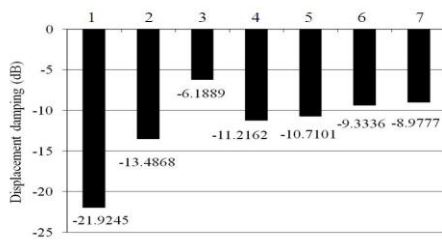


Fig.10 The values of displacement damping for different excitation forces using MsM-based semi-active pulse-switching technique:
 (1) harmonic 1st mode, (2) harmonic 2nd mode, (3) harmonic 3rd mode (4) stationary random, (5) non-stationary random, (6) pulse and (7) random shock excitation.

According to Fig. 10, resulted damping for the 3rd mode is lower than that for the 1st mode. So, as mentioned above, using a PCLD layer in addition to SSDC technique compensates this reduction. In the following, numerical results for simultaneous use of SSDC method and PCLD layer are presented. Free end deflection signals for harmonic excitation with 1*N* amplitude and with the first three resonance frequencies of the system in the case of uncontrolled, PCLD control, SSDC control and SSDC/PCLD hybrid technique are presented in Figs. 11 to 13. As shown in Fig. 11 for the first mode, the MsM-based SSDC technique suppresses system vibrations very well but PCLD layer doesn't affect significantly on vibrations amplitude. By increasing excitation frequency in Figs. 12 and 13, the importance of PCLD layer for vibration suppression becomes more visible, especially for the third mode. As shown in Fig. 13, SSDC technique efficiency reduction is compensated by PCLD layer. Resulted damping for the first three modes are presented in Fig. 14. As shown in this figure, the resulted damping for hybrid MsM-based SSDC pulse-switching technique with PCLD layer provides significant damping in both low and high frequencies.

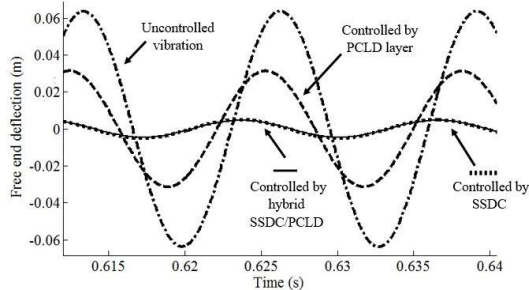


Fig.11 Free end deflection of the beam under harmonic excitation with the 1st resonance frequency, — Controlled by hybrid SSDC/PCLD, Controlled by SSDC, - - - - - Controlled by PCLD layer, - · - · - · Uncontrolled.

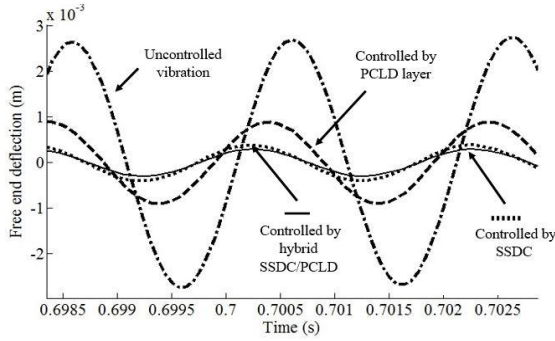


Fig.12 Free end deflection of the beam under harmonic excitation with the 2nd resonance frequency, — Controlled by hybrid SSDC/PCLD, Controlled by SSDC, -.-.-.- Controlled by PCLD layer, - - - - - Uncontrolled.

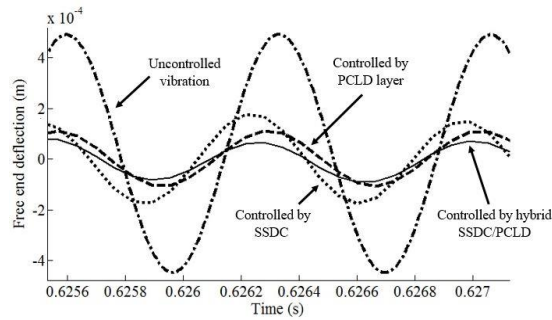


Fig.13 Free end deflection of the beam under harmonic excitation with the 3rd resonance frequency, — Controlled by hybrid SSDC/PCLD, Controlled by SSDC, -.-.-.- Controlled by PCLD layer, - - - - - Uncontrolled.

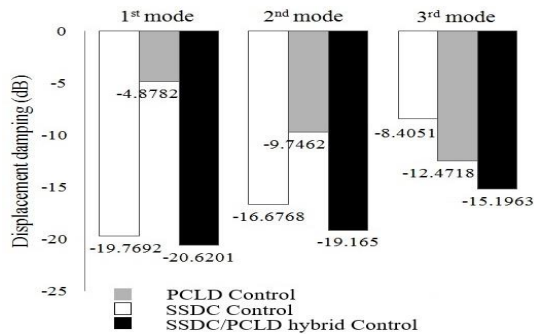


Fig.14 Resulted displacement damping for different control techniques under harmonic excitations for the first three bending modes.

7 CONCLUSIONS

The magnetostrictive-based semi-active SSDC pulse-switching control technique is introduced in this paper. The most famous actuators for vibration control are piezoelectric materials. Many control techniques such as passive, active and semi-active methods are developed using these materials. Compared with piezoelectric-based, magnetostrictive-based control methods have higher coupling efficiency, higher Curie temperature, higher flexibility to be integrated with curved structures and no depolarization problems (because magnetostriction is an inherent material property). The best vibration control methods using smart actuators are semi-active approaches that are as strong as active methods and needs no external energy supply such as passive ones. Semi-active methods are well developed for piezoelectrics but not for magnetostrictive-based ones. The aim of this work is to find a powerful semi-active control method using magnetostrictive materials.

The proposed SSDC method is introduced as a completely new semi-active vibration control technique using magnetostrictives in comparison with piezoelectric-based methods. SSDC method needs no external energy supply and uses system mechanical energy to control vibrations. This method is interesting for structural damping applications for almost all excitation types, because it provides simultaneously good damping performance, great robustness, good stability and very low power requirements.

The results show that SSDC/PCLD hybrid control provides significant damping at both low and high frequencies.

ACKNOWLEDGMENTS

The authors convey their sincere thanks to Dr. Arash Ahmadi from Windsor University for technical support in electronic part of this work.

REFERENCES

- [1] Davis C.L., Lesieutre G.A., 2000, An actively tuned solid-state vibration absorber using capacitive shunting of piezoelectric stiffness, *Journal of Sound and Vibration* **232**: 601-617.
- [2] Rao M.D., 2003, Recent applications of viscoelastic damping for noise control in automobiles and commercial airplanes, *Journal of Sound and Vibration* **262**: 457-474.
- [3] Hongli J., Jinhao Q., Kongjun Z., 2010, Vibration control of a composite beam using self-sensing semi active approach, *Chinese Journal of Mechanical Engineering* **23**: 663.
- [4] Corr L.R., Clark W.W., 2003, A novel semi-active multi-modal vibration control law for a piezoceramic actuator, *Transactions of the ASME* **125**: 214-222.
- [5] Guyomar D., Richard C., Mohammadi S., 2007, Semi-passive random vibration control based on statistics, *Journal of Sound and Vibration* **307**(3-5): 818-833.
- [6] Clark W.W., 1999, Semi-active vibration control with piezoelectric materials as variable stiffness, actuators, *Proceedings of SPIE International Symposium on Smart Structures and Materials: Passive Damping and Isolation*, Newport Beach, USA.
- [7] Badel A., Sebald G., Guyomar D., Lallart M., Lefeuvre E., Richard C., Qiu J., 2006, Piezoelectric vibration control by synchronized switching on adaptive voltage sources: Towards wideband semi active damping, *Journal of Acoustics Society American* **119**: 2815-2825.
- [8] Honhli J., Qiu J., Badel A., 2009, Semi active vibration control of a composite beam using an adaptive SSDV approach, *Journal of Intelligent Material Systems and Structures* **20**(3): 401-412.
- [9] Singhal A., Sahu S. A., Chaudhary S., 2018, Approximation of surface wave frequency in piezo-composite structure, *Journal of Composites Part B* **144**: 19-28.
- [10] Singh M. K., Sahu S. A., Singhal A., Chaudhary S., 2018, Approximation of surface wave velocity in smart composite structure using Wentzel–Kramers–Brillouin method, *Journal of Intelligent Material Systems and Structures* **29**(18): 3582-3597.
- [11] Singhal A., Sahu S. A., Chaudhary S., 2018, Liouville–Green approximation: An analytical approach to study the elastic waves vibrations in composite structure of piezo material, *Journal of Composite Structures* **184**: 714-727.
- [12] Kumar J.S., Ganesan N., Swarnamani S., Padmanabhan C., 2003, Active control of beam with magnetostrictive layer, *Journal of Computers and Structures* **81**: 1375-1382.
- [13] Hernando A., Vazquez M., Barandiaran J.M., 1988, Metallic glasses and sensing applications, *Journal of Physics E-Scientific Instruments* **21**(12): 1129-1139.
- [14] Savage H.T., Spano M.L., 1982, Theory and application of highly magnetoelastic Metglas 2605SC, *Journal of Applied Physics* **53**(11): 8092-8097.
- [15] Huang J., O'Handley R.C., Bono D., 2003, New, high-sensitivity, hybrid magnetostrictive/electroactive magnetic field sensors, *Proceedings of SPIE* **5050**: 229-237.
- [16] May C., Kuhn K., Pagliaruolo P., Janocha H., 2003, Magnetostrictive dynamic vibration absorber (DVA) for passive and active damping, *Proceedings of Euronoise*, Naples, Italy.
- [17] Kumar J.S., Ganesan N., Swarnamani S., Padmanabhan C., 2003, Active control of cylindrical shell with magnetostrictive layer, *Journal of Sound and Vibration* **262**: 577-589.
- [18] Moon S.J., Lim C.W., Kim B.H., Park Y., 2007, Structural vibration control using linear magnetostrictive actuators, *Journal of Sound and Vibration* **302**: 875-891.
- [19] Bartlet P.A., Eaton S.J., Gore J., Metheringham W.J., Jenner A.G., 2001, High-power, low frequency magnetostrictive actuation for anti-vibration application, *Journal of Sensors and Actuators* **91**: 133-136.
- [20] Zhang T., Jang C., Zhang H., Xu H., 2004, Giant magnetostrictive actuators for active vibration control, *Journal of Smart Material and Structures* **13**: 473-477.
- [21] Braghin F., Cinquemani S., Resta F., 2011, A model of magnetostrictive actuators for active vibration control, *Journal of Sensors and Actuators* **165**: 342-350.
- [22] Krishna Murty A.V., Anjanappa M., Wu Y. F., 1997, The use of magnetostrictive particle actuators for vibration attenuation of flexible beams, *Journal of Sound Vibration* **206**: 133-149.
- [23] Reddy J.N., Barbosa J.I., 1999, Vibration suppression of composite laminates with magnetostrictive layers, *Proceedings of the International Conference on Smart Materials, Structures and Systems*, Bangalore, India.
- [24] Dapino M.J., 2004, On magnetostrictive materials and their use in adaptive structures, *Journal of Structural Engineering and Mechanics* **17**(3-4): 303-329.
- [25] Mohammadi S., Hatam S., Khodayari A., 2013, Modelling of a hybrid semi- active/passive vibration control technique, *Journal of Vibration and Control* **21**: 21-28.

- [26] Wang L., 2007, *Vibration Energy Harvesting by Magnetostrictive Materials for Powering Wireless Sensors*, Ph.D Thesis, North Carolina State University.
- [27] Naem W., 2009, *Concepts in Electronic Circuits*, Ventus Publishing ApS.
- [28] Alam P., Kundu S., Gupta S., 2017, Dispersion and attenuation of torsional wave in a viscoelastic layer bonded between a layer and a half-space of dry sandy media, *Journal of Applied Mathematics and Mechanics* **38**(9):1313-1328.
- [29] Kundu S., Alam P., Gupta S., Pandit D. Kr., 2017, Impacts on the propagation of SH-waves in a heterogeneous viscoelastic layer sandwiched between an anisotropic porous layer and an initially stressed isotropic half space, *Journal of Mechanics* **33**(1): 13-22.
- [30] Alam P., Kundu S., Gupta S., 2018, Dispersion and attenuation of love-type waves due to a point source in magneto-viscoelastic layer, *Journal of Mechanics* **34**(6): 801-816.
- [31] Saidi I., Gad E. F., Wilson J. L., Haritos N., 2008, Innovative passive viscoelastic damper to suppress excessive floor vibrations, *Australian Earthquake Engineering Society Conference*.
- [32] Cremer L., Heckl M., 1988, *Structure-Borne Sound*, Springer-Verlag Press, New York.
- [33] Dewangan P., 2009, *Passive Viscoelastic Constrained Layer Damping for Structural Application*, M.Sc Thesis, National Institute of Technology Rourkela.
- [34] Marsh E.R., Hale L.C., 1998, Damping of flexural waves with imbedded viscoelastic materials, *Journal of Vibration and Acoustics* **120**: 188-193.
- [35] Rongong J.A., Wright J.R., Wynne R.J., Tomlinson G.R., 1997, Modeling of a hybrid constrained layer/piezoceramic approach to active damping, *Journal of Vibration and Acoustics* **119**: 120-130.
- [36] Staley M.H., 2005, *Development of a Prototype Magnetostrictive Energy Harvesting Device*, M.Sc Thesis, University of Maryland.